Chapter 16
TOCSY

Timothy D. W. Claridge

Chemistry Research Laboratory, Department of Chemistry, University of Oxford, Mansfield Road, Oxford OX1 3TA, UK

16.1 INTRODUCTION

The homonuclear TOCSY experiment[1] provides one of the most powerful methods for establishing the presence of scalar (J) coupling between nuclei in a molecule (typically protons, on which this article focuses). Its ability to trace correlations between protons means that it is closely related to the COSY experiment (see Chapters 12 and 13) and indeed the 2D TOCSY has a similar overall appearance to 2D COSY. Although COSY presents correlations which arise from coherence transfer between spins that share scalar couplings, TOCSY extends this idea by being able to propagate the transfer of polarization throughout a network of coupled spins by virtue of a continuous sequence of scalar-coupled nuclei. Thus, for a sequence in which proton A scalar couples to B, B to C, and C to D, one would expect to observe isolated cross peaks between each spin pair representative of these couplings in the corresponding 2D COSY experiment (Figure 16.1a). In TOCSY, it becomes possible to transfer polarization in a stepwise manner from proton A, on to B, then C, then D along the spin-coupled network such that in the final 2D TOCSY one would observe correlations from proton A to B, C, and D simultaneously (Figure 16.1b). This ability to propagate polarization along networks of spins and correlate their interactions gives rise to the title of this method. The information content of TOCSY is accordingly greater than that of COSY and is often used in addition to COSY for the definition of proton-coupling interactions in the analysis of more complex spectra. Its ability to group together isolated networks of coupled spins enables one to break down complex correlation spectra into smaller subsections that may then be correlated with discrete parts of a molecular structure, as illustrated later in the article. Not surprisingly, the method has found widespread application to molecules that are intrinsically composed of isolated groups of coupled spins. Common examples of this include the analysis of peptides in which individual amino acids may be identified in their entirety or (oligo)saccharides wherein protons within each sugar unit may be correlated. The method also proves invaluable in the elucidation of complex organic structures such as natural products for which resonance overlap can lead to ambiguity in the analysis of COSY correlations. The ability to elicit further transfers between protons can often reveal more remote correlations that may then overcome the troublesome bottleneck in the assignment process caused by peak overlap. The extent to which

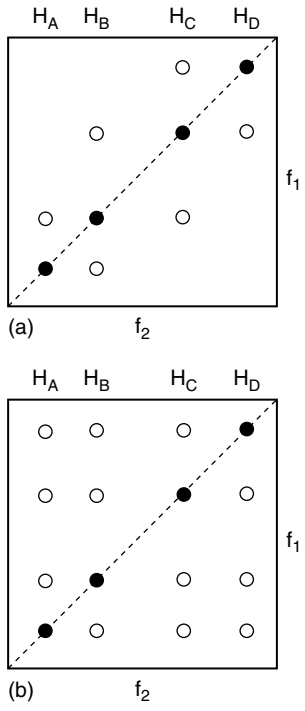

Figure 16.1. Schematic 2D spectra showing the correlations expected between protons A, B, C, and D for (a) 2D COSY and (b) 2D TOCSY.

polarization is transferred along a network of coupled nuclei is dictated, at least in part, by the duration of the so-called mixing sequence used within the experiment. Although something of an oversimplification, one can, to a reasonable approximation, correlate the number of polarization transfer steps with the total duration of the mixing sequence, as will be considered in what follows, with longer mixing periods generally enabling transfer to more remote partners. Variation of this mixing duration offers the operator some degree of control over the extent of transfer between spins and allows the experiment to be tuned to explore spin coupling networks.

Although originally conceived as a 2D experiment and still very widely used in this form, TOCSY is also often applied as a selective 1D variant for the study of midsized organic molecules in the areas of synthetic or natural product chemistry. This enables one to extract and examine in detail smaller regions of the complete proton spectrum under high resolution conditions. In particular, modern selective methods incorporating pulsed field gradients are able to provide very clean selective 1D spectra, which can reveal multiplet structures that were otherwise completely buried in the parent 1D proton spectrum and thus not accessible for interpretation. Thus, both 2D and 1D variants now find widespread application in chemical and biochemical laboratories and are considered after the principles and practical realization of the TOCSY experiment have been described.

16.2 PRINCIPLES

16.2.1 The Pulse Sequence

The principles underlying the execution of the 2D TOCSY experiment closely follow those applicable to 2D COSY, and the TOCSY sequence (Figure 16.2) can be described as comprising the usual elements of any 2D experiment: preparation–evolution–mixing–detection. The first two elements allow for initial excitation and frequency labeling during the t_1 evolution period as for any homonuclear 2D sequence and we do not consider these aspects further here (see Chapter 12). The fundamental element of TOCSY that sets it apart from COSY is the subsequent influence of the mixing scheme it employs. It is during this period that the transfer of polarization (coherence) among networks of coupled spins occurs during a mixing time of duration τ_m before the usual t_2 detection period. Although in COSY the mixing element typically comprises a single pulse (usually corresponding to a pulse tip angle in the region of 45–90°), the mixing sequence used for TOCSY comprises an extended sequence of pulses designed to produce the desired multistep transfers. The sequence is usually referred to as an

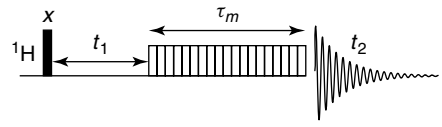

Figure 16.2. The basic 2D TOCSY sequence. Following initial excitation and frequency labeling during t_1, magnetization is then subjected to an isotropic mixing period of duration τ_m (shown as hashed box) before detection during t_2. The solid bar indicates a 90° pulse with phase shown above (a similar convention is used in all subsequent pulse sequences).

isotropic mixing scheme and we first consider the operation of this in a more formal context, followed by a more descriptive version of events.

16.2.2 Isotropic Mixing

The influence of an isotropic mixing scheme may be described by the consideration of the relevant Hamiltonian operator. Under the usual conditions of evolution of weakly coupled spins in the absence of a mixing scheme, this may be described as

$$\widehat{H} = \sum_i -\omega_i \hat{I}_{iz} + \sum_{i \neq j} 2\pi J_{ij} \hat{I}_{iz} \hat{I}_{jz} \qquad (16.1)$$

in which the first term represents the chemical shift terms and the second the scalar spin coupling terms. Under the influence of an effective isotropic mixing scheme, this reduces to

$$\widehat{H}_J = \sum_{i \neq j} 2\pi J_{ij} \ \hat{I}_{iz} \hat{I}_{jz} \qquad (16.2)$$

in which *only* the scalar coupling terms are operative. Now, consider the influence of this Hamiltonian when applied for a mixing period τ_m to a system containing just two coupled protons, 1 and 2, which share a scalar coupling J_{12}. The effect on the evolution of longitudinal (z) magnetization on spin 1 is

$$\begin{aligned} \hat{I}_{1z} \xrightarrow{\widehat{H_J}\tau_m} & \tfrac{1}{2}\left[1 + \cos(2\pi J_{12}\tau_m)\right] \hat{I}_{1z} \\ & + \tfrac{1}{2}\left[1 - \cos(2\pi J_{12}\tau_m)\right] \hat{I}_{2z} \\ & - \tfrac{1}{2}\sin(2\pi J_{12}\tau_m)(2\hat{I}_{1y}\hat{I}_{2x} - 2\hat{I}_{1x}\hat{I}_{2y}) \end{aligned} \qquad (16.3)$$

We see in the second term that some element of z-magnetization originating on spin 1 ($\hat{I}_{1z}$) has transferred to become z-magnetization on spin 2 ($\hat{I}_{2z}$), to an extent that depends upon the magnitude of J_{12} and the duration τ_m. Furthermore, complete transfer from spin 1 to spin 2 occurs after a period $1/(2J_{12})$ s. In a two-spin system such as this, it may also be noted that the use of a mixing time greater than this will lead to transfer back from spin 2 onto spin 1 once more, and so on, and this oscillatory transfer of magnetization between spins is characteristic of isotropic mixing schemes (Figure 16.3). In systems where further spin coupling exists, such transfer can extend to other coupled partners and, although the details of these processes become more complex, the notion of oscillatory transfer between spins still prevails, yielding the extended transfers throughout spin-coupled networks described above.

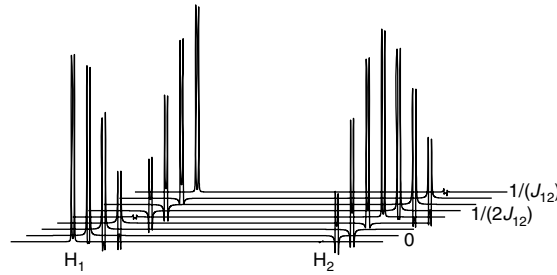

Figure 16.3. The transfer of magnetization between two scalar-coupled spins during isotropic mixing. Magnetization initially on spin 1 undergoes an oscillatory transfer between spins 1 and 2 as a function of the applied mixing time τ_m.

Further consideration of the terms in equation (16.3) shows that there is a *net* transfer of *in-phase* magnetization between spins ($\hat{I}_{1z} \rightarrow \hat{I}_{2z}$). This is in contrast to the results of coherence transfer occurring in the COSY experiment in which it is the transfer of *antiphase* magnetization that occurs (such as $\hat{I}_{1y} \rightarrow \hat{I}_{1z}\hat{I}_{2x}$). In practical terms, this can mean that in situations where resonance linewidths become large relative to the homonuclear coupling constants, TOCSY may become the favored experiment over COSY, which can suffer reduced sensitivity arising from cancellation of antiphase terms. The in-phase transfer associated with TOCSY also means that data may be processed to yield both diagonal and cross peaks displaying the favored double absorption lineshapes. However, we must also consider the third term in equation (16.3), which we have so far conveniently ignored and which represents the unwelcome generation of zero-quantum coherence during the mixing sequence, the intensity of which is also time dependent. This term ultimately gives rise to antiphase terms that contribute to both diagonal and cross peaks and these are orthogonal to the desired in-phase peaks. These will, therefore, produce highly undesirable antiphase *dispersive* contributions to peaks that may compromise resolution and are, therefore, generally considered artifacts of the isotropic mixing scheme. These appear in the traces of Figure 16.3 as phase distortions to the otherwise in-phase peaks. In some cases, their active removal is considered beneficial and this aspect is considered in 16.3.4.

The mixing scheme is termed *isotropic* because when one considers the influence of the scheme on x- and y-magnetization, similar terms may also be derived:

$$\hat{I}_{1x} \xrightarrow{\widehat{H_J}\tau_m} \tfrac{1}{2}\left[1 + \cos\left(2\pi J_{12}\tau_m\right)\right]\hat{I}_{1x} + \tfrac{1}{2}\left[1 - \cos\left(2\pi J_{12}\tau_m\right)\right]\hat{I}_{2x} - \tfrac{1}{2}\sin\left(2\pi J_{12}\tau_m\right)\left(2\hat{I}_{1z}\hat{I}_{2y} - 2\hat{I}_{1y}\hat{I}_{2z}\right) \tag{16.4}$$

$$\hat{I}_{1y} \xrightarrow{\widehat{H_J}\tau_m} \tfrac{1}{2}\left[1 + \cos\left(2\pi J_{12}\tau_m\right)\right]\hat{I}_{1y} + \tfrac{1}{2}\left[1 - \cos(2\pi J_{12}\tau_m)\right]\hat{I}_{2y} - \tfrac{1}{2}\sin\left(2\pi J_{12}\tau_m\right)\left(2\hat{I}_{1x}\hat{I}_{2z} - 2\hat{I}_{1z}\hat{I}_{2x}\right) \tag{16.5}$$

In both cases, we again see that there is a transfer of in-phase magnetization of the form $\hat{I}_{1x} \rightarrow \hat{I}_{2x}$ and $\hat{I}_{1y} \rightarrow \hat{I}_{2y}$, meaning that mixing is equally effective along all three axes. In general, the simultaneous transfer and subsequent detection of all three orthogonal z, x, and y terms will lead to spectra with complex phase properties and in the practical application of the TOCSY experiment, it is common practice to select and retain only one component to yield in-phase peak structures. Finally, note that during the transfer of x- and y-magnetization, antiphase terms are also produced (the third terms in equations (16.4) and (16.5)) and, as with the zero-quantum terms arising from z-magnetization described above, can ultimately lead to undesirable antiphase dispersive terms in the final spectrum.

16.2.3 The Hartmann–Hahn Match

As an alternative approach for describing the effect of an isotropic mixing scheme, we may consider what equations (16.1) and (16.2) represent in more descriptive terms. These imply that under the influence of mixing, the chemical shift *differences* between all protons in a spin system are effectively suppressed, but the coupling between these spins remains operational. In other words, the mixing scheme results in the spins experiencing the same effective local field, which in turn forces the protons to behave as a very strongly coupled spin system. Under such conditions, one may consider the protons to lose their unique identity (they are said to take part in collective spin modes) and share their magnetization through oscillatory exchange. The condition under which two nuclei A and X experience identical local fields as a result of the mixing scheme is known as the *Hartmann–Hahn match*, which may be defined as

$$\gamma_{(A)}B_{1(A)} = \gamma_{(X)}B_{1(X)} \tag{16.6}$$

where $\gamma_{(A)}$ and $\gamma_{(X)}$ are the magnetogyric ratios of the coupled nuclides and $B_{1(A)}$ and $B_{1(X)}$ are the applied RF fields experienced by each. In the case of a homonuclear system, the γ terms are identical and it is then a sufficient requirement that the local RF fields experienced by each spin are matched to allow transfer between them to occur. It is this alternative description of conditions suitable for polarization transfer among coupled protons that led to the alternative name of homonuclear Hartmann–Hahn spectroscopy (HOHAHA) for this experiment.[2,3] Both TOCSY and HOHAHA have been used interchangeably in the literature over the years, often dependent upon which precise form of the experiment has been implemented, but now TOCSY appears to have become the accepted name for this technique. Equation (16.6) also suggests that magnetization exchange between differing nuclides is also possible if the applied RF fields are matched according to the relevant magnetogyric ratios of the nuclides, so-called heteronuclear cross-polarization, although this approach is not widely employed in solution NMR spectroscopy and so is not discussed further (cross-polarization does, however, play a very important role in solid-state NMR spectroscopy).

16.3 PRACTICAL IMPLEMENTATION

Having addressed the fundamental principles that underlie the TOCSY experiment, we now consider the practical aspects associated with executing the experiment. We consider the requirements of a scheme suitable for isotropic mixing and some of the common variants that find widespread use and how these may be employed within working sequences. The influence of mixing times on the appearance of spectra and the most common artifacts associated with TOCSY are described, along with methods designed to suppress these artifacts.

16.3.1 Mixing Schemes

One of the simplest schemes suitable for isotropic mixing is a series of closely spaced 180° pulses repeated a sufficient number of times to achieve the desired total mixing period τ_m. However, in practice, this simple scheme performs poorly owing to the poor off-resonance performance of each 180° pulse, meaning that the efficiency of mixing degrades significantly for spins that resonate far from the applied RF. Since in most cases the RF (B_1) field is applied at the center of the spectral window, the transfer efficiency falls toward the edges of the spectrum. The limited performance of 180° pulses is a widespread limitation in many pulse experiments and the common solution to compensate these deficiencies is to replace single 180° pulses with *composite pulses* of equivalent net rotation and a similar approach lies at the heart of all common TOCSY mixing schemes. The principles involved in selecting these schemes closely parallel those used in the design of heteronuclear composite pulse decoupling (CPD) sequences and, in fact, most of the mixing schemes in use have been derived from the original CPD schemes. As with CPD, the basic composite 180° pulses are grouped into clusters of pulse cycles and supercycles in which the phases of the component pulses are stepped to provide compensation for errors (in phase or net tip angle) generated by individual composite pulses (Table 16.1). This is so that these errors do not accumulate through the repeated application of the composite pulse, thereby degrading its effectiveness. As an illustration, one of the early mixing schemes was based on the MLEV-16 CPD cycle in which each 180°_x pulse was replaced with a composite pulse of the general form $90_{-y}180_x90_{-y}$, which was then grouped as a cluster of 16 composite pulses in the compensating supercycle.[4] The off-resonance behavior of this simple composite pulse relative to a single 180° inversion pulse is illustrated in Figure 16.4, which clearly demonstrates its improved performance for off-resonance inversion with vector trajectories finishing closer to the $-z$ axis. The total mixing time may be achieved by continuous and repeated application of the MLEV-16 cycle. An alternative mixing scheme is the WALTZ-16 scheme (Table 16.1), which itself finds widespread use in proton decoupling of heteronuclear spectra.[5,6] The most efficient of the widely employed mixing schemes is the DIPSI-2 sequence, which represents the method of choice for the acquisition of proton homonuclear

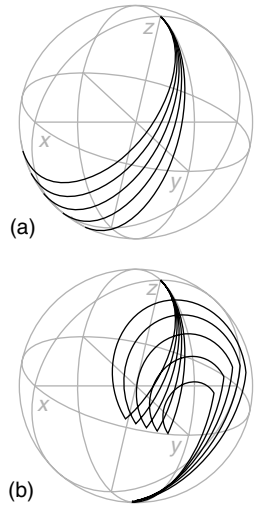

Figure 16.4. The inversion performance of (a) a single 180°_x pulse versus (b) a composite $90_x180_y90_x$ pulse as a function of resonance offset. The simulated trajectories are shown for offsets relative to the applied RF (B_1) field of 0.2, 0.3, 0.4, 0.5, and 0.6 γB_1.

TOCSY spectra.[7] This rather more elaborate scheme (Table 16.1) was again originally designed as a CPD sequence[8] but with specific consideration of the influence of homonuclear proton couplings and proves to be more effective at retaining scalar coupling terms across a wider bandwidth during the mixing period. For DIPSI-2 the effective bandwidth is comparable to the strength of the applied RF field ($\gamma B_1/2\pi$ Hz) so that a 10 ppm bandwidth at 600 MHz demands a corresponding 6 kHz RF field (90° pulse $\sim$ 42 μs). Because of the application of mixing schemes for many tens of milliseconds (as described below), it is a common practice to attenuate pulse powers during the mixing period and RF fields of around 10 kHz (corresponding to $90^\circ = 25$ μs) are commonly employed, meaning that efficient mixing over the full proton bandwidth can be readily achieved.

16.3.2 Practical Sequences

16.3.2.1 2D TOCSY

As alluded to in discussions above, practical sequences for achieving 2D TOCSY spectra displaying pure phase lineshapes require that only a single

Table 16.1. Pulse elements of common composite pulse mixing sequences used in TOCSY.

Mixing scheme	Composite 180° pulse, R	Pulse cycle	Pulse supercycle
MLEV-16	$90_{-y}180_{x}90_{-y}$	$R\overline{R}\,\overline{R}R$	$R\overline{R}\,\overline{R}\,R\overline{R}\,\overline{R}RR\overline{R}RR\overline{R}\,RR\overline{R}\,\overline{R}$
MLEV-17	$90_{-y}180_{x}90_{-y}$	$R\overline{R}\,\overline{R}R$	$R\overline{R}\,\overline{R}R\overline{R}\,\overline{R}RR\overline{R}RR\overline{R}\,RR\overline{R}\,\overline{R}180_{x}$
WALTZ-16	$270_{x}360_{-x}180_{x}270_{-x}90_{x}180_{-x}360_{x}180_{-x}270_{x}$	$R\overline{R}\,\overline{R}R$	$R\overline{R}\,\overline{R}R$
DIPSI-2	$320_{x}410_{-x}290_{x}285_{-x}30_{x}245_{-x}375_{x}265_{-x}370_{x}$	$R\overline{R}\,\overline{R}R$	$R\overline{R}\,\overline{R}R$

Units represent pulse tip angles (in degrees) with subscripts indicating relative pulse phases. The overbar represents phase inversion of all pulses.

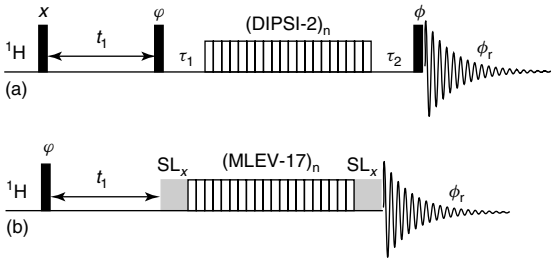

Figure 16.5. Experimental sequences for 2D TOCSY based on (a) DIPSI-2 and (b) MLEV-17 mixing. Solid bars indicate 90° pulses of indicated phase and ϕ_r the receiver phase. The periods τ_1 and τ_2 are short delays and SL represents short spin-lock purge pulses (see text). The phase ϕ is cycled $x, y, -x, -y$ along with the receiver phase to select longitudinal magnetization and phase φ is independently cycled $x, -x$ again with the receiver to cancel axial peaks. For (b) all phases, including those of the mixing sequence, are additionally cycled through $x, y, -x, -y$ along with the receiver.

component of magnetization be retained for detection during t_2. It is a common practice to select the z-component (which has more favorable relaxation behavior than transverse elements) and the standard sequence for this is shown in Figure 16.5(a).[7,9,10] In this, the mixing sequence is bracketed by two 90° pulses that serve to place magnetization along the $\pm z$ axis before the mixing stage and return this to the transverse plane for detection when mixing is completed. The delays τ_1 and τ_2 may be kept sufficiently short to allow simply for RF power switching or may be utilized to suppress artifacts arising from zero-quantum coherences, as described in 16.3.4. Phase cycling of the last 90° pulse and of the receiver through $x, y, -x$, and $-y$ selects for the desired longitudinal magnetization. Independent cycling of either the first or second 90° pulse and of the receiver through $x, -x$ is employed to remove the so-called *axial peaks* (artifacts that arise from longitudinal magnetization that exists or develops during t_1 and is therefore not frequency labeled in this dimension, hence appearing at zero f_1 frequency in the final spectrum). Additional cycling of the first 90° pulse is required according to the chosen f_1 quadrature detection scheme for phase-sensitive display (States, TPPI, or States-TPPI). The 90° pulses are applied at high power, whereas those comprising the DIPSI-2 scheme are applied at reduced power as noted above (typically $\gamma B_1/2\pi \sim 10$ kHz) and the total mixing time defined by the number of DIPSI-2 cycles completed.

Figure 16.5(b) shows an alternative implementation of TOCSY that has also found widespread use in the literature and employs a variant of the MLEV-16 scheme for eliciting the transfer of, in this case, transverse magnetization. In this method, it was found advantageous to add a single 180° purge pulse to the end of each MLEV-16 cycle to remove the effects of pulse imperfections arising during its application, giving rise to the so-called MLEV-17 scheme[3] (Table 16.1). Thus, the phase errors resulting from a complete MLEV-16 cycle will result in magnetization vectors not aligning with the $\pm x$-axis at the end of the cycle. The addition of the 180° pulse inverts the signs of the errors so that after an even number of MLEV-17 cycles the errors are cancelled and do not accumulate. The use of a purging 60° pulse instead of the 180° pulse provides for similar compensation and also finds use in this variant. The application of mixing in this way fulfills the Hartmann–Hahn match condition described above (the sequence has been described as being *energy matched* rather than *isotropic*[11]) and so provides effective polarization transfer between spins. In this implementation (originally known as *HOHAHA*), it becomes necessary to purge unwanted orthogonal transverse magnetization components so that pure phase absorption mode spectra may be displayed. This may be achieved through

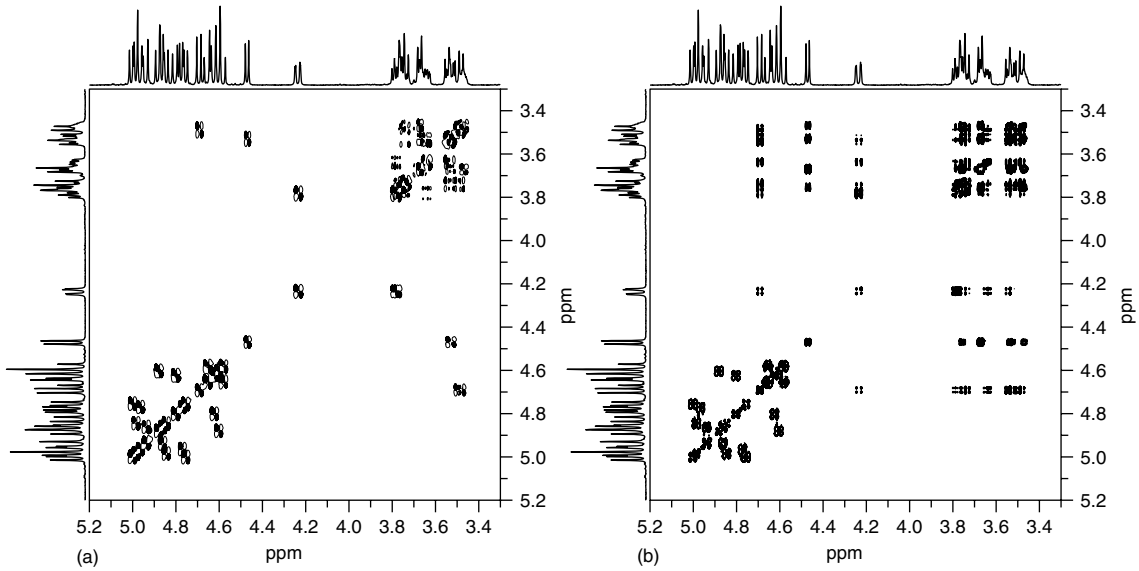

Figure 16.6. Comparison of the 500 MHz (a) COSY (as the double-quantum filtered variant) and (b) TOCSY 2D spectra of the synthetic disaccharide 1. The TOCSY experiment was collected using DIPSI-2 mixing for 150 ms.

the use of short *spin-lock* or *trim* pulses applied before and after the mixing period that serve to dephase any components not aligned with the applied RF field, thus retaining only one transverse component, as required. The trim pulses are typically only 2–3 ms in duration and are applied at the same power as the mixing scheme itself.

As suggested above, additional modifications of these sequences can be made to improve the overall appearance of the spectra, although for routine use the sequences presented here usually prove robust, efficient, and suitable for most studies. Modifications for the removal of specific artifacts are described in 16.3.4.

The 2D COSY and TOCSY experiments for the protected synthetic disaccharide **1** are compared in Figure 16.6. The presence of relayed correlations throughout the two separate saccharide ring systems is clearly revealed and results from the propagation of polarization during the 150 ms mixing period. For both ring systems, total correlations throughout each may be identified; this is most apparent in the correlations originating from the two anomeric (H1) protons at 4.69 and 4.46 ppm. The ability to extract such additional correlation information relative to the COSY experiment makes TOCSY an extremely powerful tool in spectral assignment and structure elucidation.

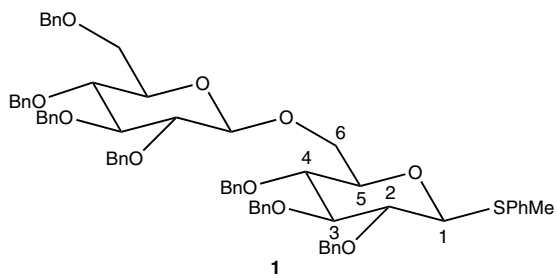

1

16.3.2.2 1D TOCSY

Although the traditional application of the TOCSY experiment has been as the 2D variant, the availability of very efficient selective excitation schemes based on pulsed field gradient selection methods means that the 1D variant of TOCSY has become a popular tool for the study of complex organic structures. As for any selective variant of a 2D sequence, it offers the potential advantage of high resolution 1D data sets that are able to reveal greater detail and of faster data acquisition when specific aspects of structure elucidation require investigation. Of particular value is the scheme in which artifacts arising from zero-quantum terms are suppressed (see below), revealing multiplet

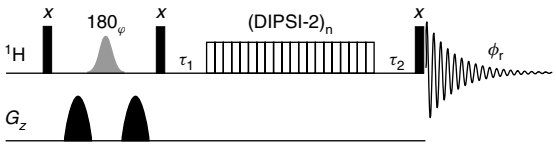

Figure 16.7. An experimental scheme for 1D selective TOCSY experiments using DIPSI-2. The selective excitation element uses a single gradient echo before the mixing period that incorporates the selective 180° pulse on the target resonance. The phase of this (φ) is cycled following the EXORCYCLE scheme to retain only magnetization originating from the selected spin.

structures with high fidelity. The resulting 1D spectrum of a selective experiment equates to the high resolution version of a 2D trace extracted through the diagonal peak corresponding to the selectively excited proton. Examples of this are given below, so here we focus on the details relevant to the pulse sequence. In essence, all that is required is to replace the frequency labeling elements of the 2D sequence with a suitable excitation scheme such that only a single target multiplet is selectively excited. A suitable sequence for this based on excitation with a single gradient echo scheme is shown in Figure 16.7. In the selective excitation scheme, all transverse proton magnetization generated by the initial 90° pulse experiences net dephasing imposed by the two equal gradient pulses (G_z) *except* that which is inverted by the selective 180° pulse for which the influence of the two gradient pulses cancels. Magnetization that survives this selection step is then utilized as the source for subsequent polarization transfer, with all other peaks appearing in the final spectrum having originated from this magnetization. The selective 180° pulse is phase cycled through x, y, $-x$, and $-y$ as the receiver is phase alternated (x, $-x$) (the EXORCYCLE sequence[12]) to ensure that only magnetization that originated from the selected spin contributes to the final spectrum.

16.3.3 Influence of Mixing Times

One of the useful features of TOCSY that can be exploited to good effect is the time dependence of the propagation of polarization along a scalar-coupled spin network. As mentioned, this process has a complex dependence on mixing time and coupling constants,[13] meaning that, in practice, one tends not to be able to precisely control the transfer process in a multispin system. Furthermore, the presence of rather small coupling constants in the chain leads to slower propagation and can act as a bottleneck in the transfer to more remote spins in the network, to the limit where couplings that reduce to zero will serve to block further transfer. Nevertheless, the general and qualitative notion of extended transfers occurring when longer mixing times are employed proves useful in structure elucidation with mixing times typically ranging from 20 up to 200 ms. This concept may be illustrated by considering the transfer of polarization in the disaccharide **1** introduced above. Figure 16.8 shows selective 1D TOCSY data recorded with DIPSI-2 mixing for periods of 10–120 ms in which the progressive propagation of magnetization from the selected source spin of H1 to more remote spins is increasingly apparent. Thus, for $\tau_m \leq 20$ ms only a single step transfer is seen, when approximately 40–60 ms transfers over 2–3 steps become apparent, from 80–100 ms 4–5 step transfer appears, and by $\tau_m = 120$ ms transfer over 5 steps from H1 through to the H6 protons are readily identified (these extended correlations are as seen in the 2D TOCSY data shown in Figure 16.6). The time dependence of the transfer is also illustrated in Figure 16.9, which shows the integrated peak intensities from the 1D spectra of Figure 16.8. The complex oscillatory behavior among the spins is apparent with a tendency toward a more even distribution of magnetization across the whole spin system with longer mixing periods. The fluctuation in intensities suggests caution in the assessment of peak intensities in relation to the number of transfer steps involved, especially when only a single mixing time is employed. Finally, note that in compound **1**, the ability to transfer polarization over many steps with moderate mixing times is aided by the presence of a continuous sequence of relatively large (~10 Hz) vicinal couplings between the axial protons of the thio-glucose sugar ring, whereas in other spin systems the transfer may be rather less efficient and more restricted for similar mixing times, dependent upon the coupling constants present in the structure.

16.3.4 Zero-Quantum Artifacts

Previously we saw how zero-quantum coherences could be generated through the operation of an isotropic mixing sequence and how these could ultimately lead to the generation of undesirable antiphase

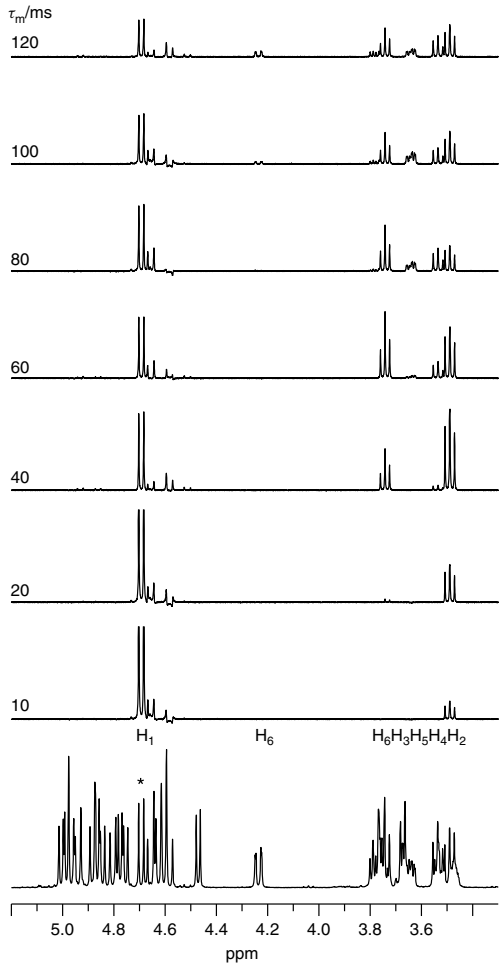

Figure 16.8. Selective 500-MHz 1D TOCSY traces recorded for disaccharide 1 as a function of mixing time τ_m. The sequence shown in Figure 16.7 was employed (but incorporating additional zero-quantum suppression as described in 16.3.4.2) and selective excitation achieved with an 80-ms Gaussian inversion pulse applied to the H1 anomeric proton of the thio-sugar unit as the source proton (shown with asterisk).

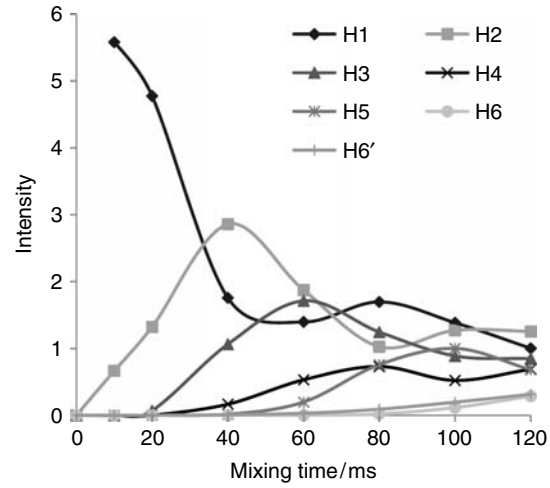

Figure 16.9. The time dependence of polarization transfer in disaccharide 1. Integrated peak intensities (arbitrary units) taken from Figure 16.8 are shown as a function of mixing time.

dispersive contributions to the final spectrum (see, for example, Figure 16.3). Such contributions are considered artifacts as they deteriorate the quality of spectra, although for many routine applications of TOCSY these prove not too troublesome and their presence can be tolerated; being antiphase, the dispersive tails tend to cancel each other to a substantial degree. Nevertheless, in some cases, it may prove advantageous to eliminate these, such as when the highest cross-peak resolution is required in 2D spectra or when undistorted multiplet structures are demanded for inspection from selective 1D TOCSY data (Figure 16.10). This, however, proves not to be a simple task, since zero-quantum coherences are of order zero ($p = 0$) and are, therefore, insensitive to changes in RF phase or to the application of field gradient pulses. Thus, classical phase cycling techniques are unable to cancel these contributions and gradient pulses cannot purge them, thus demanding alternative approaches. The solutions presented below both make use of the fact that zero-quantum coherences are manifestations of transverse magnetization and hence will evolve during a period of free precession. The evolution rate equates to the difference in the rotating-frame frequencies of the J-coupled spins (here termed A and X), giving rise to the coherences, i.e., $\nu_{ZQC} = |\nu_A - \nu_X|$ Hz. Differing periods of precession will then lead to differing phases acquired by the coherences and so provide the potential for their cancellation through coaddition.

16.3.4.1 Z-Filtration

The suppression method based on the so-called *z-filter*[14] may be understood with reference to the TOCSY sequence shown in Figure 16.5(a), although

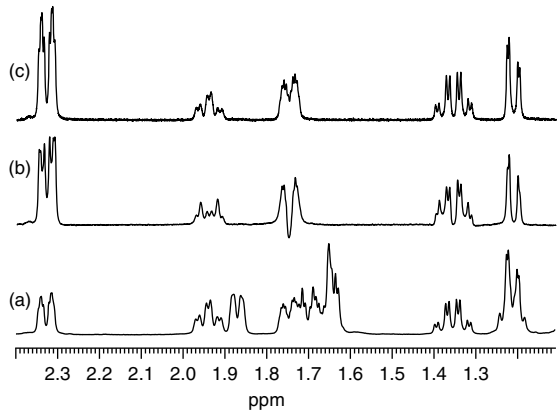

Figure 16.10. Elimination of zero-quantum coherence artifacts in TOCSY. (a) Reference 500 MHz ^{1}H spectrum (b) 1D TOCSY trace showing distortions originating from zero-quantum coherences and (c) 1D trace in which zero-quantum-derived artifacts have been eliminated. (c) The suppression was achieved using the scheme described in 16.3.4.2 with suppression elements of 10 and 15 ms employing 40 kHz adiabatic RF sweeps positioned either side of the mixing scheme.

it has wider application as a filter element in other sequences; one such example is NOESY, wherein it has a similar zero-quantum suppression role (see Chapter 18). In its most general form, it is a pulse sequence element that serves to select and retain only magnetization that exists along the z axis, as here in the case of TOCSY. As described in the sequence above, the delays τ_1 and τ_2 on either side of the isotropic mixing sequence are kept short and of fixed duration sufficient to enable spectrometer power switching. However, these may be further employed in the context of a z-filter such that one (or optimally both) adopts a sufficient duration in which zero-quantum coherences are able to evolve and so accrue an appreciable net phase angle. Consider the case in which the period τ_2 is altered and adopts two differing values in separate experiments. This will impart a differing net phase angle on the coherences for the first and second experiment and if the difference in the two time periods was such that $\Delta\tau_2 = 1/(2\nu_{ZQC})$, then the phase difference associated with the coherences from the two experiments would be 180°. The addition of the two data sets will then lead to complete cancellation of the zero-quantum terms arising between spins A and X due to their opposing phase and hence to the removal of associated artifacts in the final spectrum. For the short durations typically necessary for such z-filtration in proton TOCSY experiments, the desired z-magnetization components are largely unaffected by variation in τ_2 (or τ_1) and contribute to the final spectrum without disturbance. Thus, for the case of two coupled spins differing in shift by 0.1 ppm, a difference in evolution times $\Delta\tau_2$ of 10 ms will lead to the desired cancellation at 500 MHz, while a shift difference of 1 ppm requires a difference of only 1 ms. For other zero-quantum evolution frequencies (that is, other shift differences between coupled spins) and for the case of different spectrometer field strengths, alternative $\Delta\tau_2$ values will be appropriate to achieve such cancellation, so in a practical application, it will typically be necessary to collect experiments over a range of τ_2 periods and coadd the data to achieve an acceptable degree of suppression. This often requires the collection of 8–10 experiments with τ_2 delays varying pseudo-randomly between 2 and 20 ms.

Such an approach may be feasible in the acquisition of selective 1D data since these are typically quicker to acquire than their 2D counterparts, but the need to acquire multiple data sets can make this impractical for the collection of 2D TOCSY, notably when signal-to-noise requirements do not demand the need for such extended data acquisition. The method described below proves to be far superior in such cases, but does demand access to pulsed field gradient capabilities.

Finally, note that it is also possible to apply the method of z-filtration to TOCSY experiments that employ the MLEV-17-based sequence such as the one shown in Figure 16.5(b). Here, it becomes necessary to add the complete z-filter element of $90_x - \tau - 90_x$ after the second spin-lock pulse and to vary the τ delay as described above. The 90° pulses serve to transfer magnetization initially from and then back to the transverse plane, thus passing the desired magnetization through the filter while ultimately imposing the required elimination of antiphase terms.

16.3.4.2 ZQ Suppression

The method of zero-quantum suppression devised by Thrippleton and Keeler[15] seeks to achieve the cancellation of zero-quantum terms in a single scan and so has potentially wider application than the z-filter described above. A complete description of the method is beyond the scope of this article, so

only an overview is presented here. To appreciate its operation, we begin by introducing a slight variation of the aforementioned z-filter in which the extent of evolution of zero-quantum terms can be achieved by keeping the z-filter delay τ fixed rather than variable, but instead applying a 180° refocusing pulse within this period. The delay τ can now be described as comprising the sequence $\tau_a - 180 - \tau_b$, wherein τ_a and τ_b need not be of the same duration. Since the 180° pulse will refocus the evolution of the zero-quantum terms occurring during τ_a, net evolution of these terms is only effective for a period $|\tau_b - \tau_a|$. If a sequence of experiments were acquired in which the position of the 180° pulse varied within τ (that is, if the values of τ_a and τ_b varied while their sum remained constant), these would label the ZQ terms with different phase angles and the summation of the experiments would lead to overall ZQ cancellation, as described above. Now consider the operation of the zero-quantum suppression element itself, which comprises the simultaneous application of a frequency-modulated 180° inversion pulse of linear sweep (e.g., an adiabatic pulse) and a linear field gradient applied over the length of the sample (a z-gradient). The implementation of these elements within the z-filter delays of TOCSY is illustrated in Figure 16.11. The field gradient serves to spatially encode spins along the length of the sample in the usual manner so that the effect of the simultaneous frequency-swept pulse is to deliver refocusing to different regions or "slices" of the sample at different times within τ. The result is that zero-quantum terms associated with spin pairs that are physically located in different parts of the sample will have acquired differing net phases at the end of the sweep. If the field gradient were now removed, the superposition of the terms from spins in all parts of the sample will lead to their net cancellation. This occurs from the single application of the suppression element and hence *in a single scan* rather than from the coaddition of many separate experiments. Therefore, this presents a time-efficient means of eliminating artifacts that arise from zero-quantum coherences that can be applied to many pulse sequences, NOESY being another example.

For the method to be effective, it is necessary for the evolution period to be of sufficient duration for the zero-quantum terms to evolve (typically $\tau = 10–50$ ms) and for the frequency sweep to be matched with the frequency spread imposed by the field gradient. This requires the sequence to

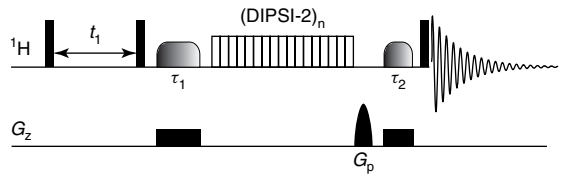

Figure 16.11. The single-scan zero-quantum suppression scheme applied to TOCSY. The shaded ^{1}H pulses represent frequency-swept inversion pulses applied simultaneously with a z field gradient and G_p a gradient purge pulse.

be calibrated, details of which may be found in the original literature.[15] When applied to TOCSY, the periods τ_1 and τ_2 may both be filtered in this manner and an additional purge gradient (G_p) may also be applied after the isotropic mixing sequence to eliminate unwanted transverse terms (with the exception of zero-quantum terms). The effectiveness of this scheme may be appreciated in the 1D TOCSY traces shown in Figure 16.10 where trace (b) employs DIPSI-2 mixing without any elimination of zero-quantum artifacts and clearly exhibits the anticipated distortions to multiplet structures arising from antiphase contributions. Trace (c) incorporates direct zero-quantum suppression and achieves the faithful reproduction of these multiplets; the spectra shown in Figure 16.8 were filtered in a similar manner.

16.3.5 Cross-Relaxation Artifacts

A quite different form of artifact that may occur in TOCSY experiments originates from dipolar cross relaxation occurring between protons during the mixing period (see Chapter 20). This can give rise to correlation cross peaks arising from the nuclear Overhauser effect rather than from polarization transfer between scalar-coupled spins. These artifacts appear either as separate additional cross peaks or may serve to cancel or reduce the intensity of genuine TOCSY correlations if coincident as they are usually of opposite sign. These arise because the TOCSY mixing sequence emulates that employed in the rotating-frame NOE (ROESY) experiment. In ROESY, the application of a period of continuous RF irradiation serves to eliminate chemical shift evolution of transverse magnetization in the rotating frame (so-called spin-locking), thus enabling cross relaxation to occur between dipolar coupled spins (see Chapter 19). During an

isotropic mixing sequence, magnetization passes between longitudinal and transverse states such that both NOE and ROE effects may develop and potentially contribute to artifacts in TOCSY. The severity of these is dependent upon the motional properties of the molecule(s) under study. For small, rapidly tumbling molecules, the cross-relaxation rates for both the NOE (σ_{NOE}) and the ROE (σ_{ROE}) are small and for the relatively short mixing times used in TOCSY, the intensity of associated artifacts is often negligible and rarely problematic. For large molecules in the slow-motion limit both rates can be high and both NOEs and ROEs can develop to appreciable intensities during TOCSY mixing periods and can compete with coherent magnetization transfer. This is most often the case in the study of bio-macromolecules, for example, and in such cases it is beneficial to eliminate the undesirable NOE/ROE contributions.

One common approach to this utilizes the fact that in the slow-motion (spin-diffusion) limit where $\omega_0\tau_c \gg 1$ (ω_0 is the resonant frequency and τ_c the rotational correlation time), the NOE and ROE are of opposite sign, providing the potential for their cancellation through coaddition. Under these conditions, $\sigma_{ROE} = -2\sigma_{NOE}$ and this relationship must be factored in when accounting for the total periods in which the ROE and NOE can develop during mixing. Thus, if magnetization spends twice as long aligned with the longitudinal direction as in the transverse plane, the cross-relaxation terms cancel. This may be achieved through the inclusion of appropriate delays within each composite pulse element that make up the TOCSY mixing sequence, so, for example, the composite pulse $90_{-y} - 180_x - 90_{-y}$ becomes $90_{-y} - \Delta - 180_x - \Delta - 90_{-y}$ in which the additional delay Δ is selected to provide the appropriate balance between periods when magnetization is longitudinal (NOE) and transverse (ROE). Under these conditions, the net cross-relaxation rate becomes zero and cross-relaxation artifacts are not generated. This gives rise to the so-called clean-TOCSY experiments, which have been derived from the original MLEV-17[16] and DIPSI-2[17] mixing sequences. More modern approaches employ shaped pulses within the mixing scheme to also reduce the total power delivered to the sample[18] or have utilized computer optimized design of mixing schemes to specifically counter the influence of cross relaxation, examples being the CITY[19] and TOWNY[20] mixing sequences. Detailed consideration of ROESY artifacts in TOCSY and of solutions to their compensation are presented in Chapter 20 and hence no further elaboration is presented here.

Similar considerations to those presented above would also suggest the potential for TOCSY artifacts appearing in ROESY spectra and this is indeed a problem for both small and large molecules. They may also be addressed through suitable modifications of the mixing schemes used for ROESY and these are likewise addressed in Chapter 20.

16.4 APPLICATIONS

TOCSY finds application in the identification of networks of scalar-coupled spins within molecules. It is especially well suited for the analysis of molecules that inherently possess isolated clusters of coupled protons such as the amino acids of polypeptides or the sugar units of oligosaccharides. The 2D TOCSY shown in Figure 16.6(b) has already demonstrated its application for the identification of discrete spin systems in a disaccharide. In the study of (unprotected) oligosaccharides, the anomeric (H1) sugar proton resonances are often resolved at high chemical shifts and present suitable points from which to establish correlations throughout each sugar unit, provided coupling constants of sufficient magnitude exist between protons for the propagation of polarization. In the study of peptides, the backbone NH protons can serve a similar purpose. Figure 16.12 shows application of TOCSY to the assignment of a 19 amino-acid peptide (biotin)-DLDLEMLAPYIPMDDDFQL collected with the MLEV-17 mixing sequence applied for a period of 80 ms to establish transfer along the amino-acid side chains. The peptide was prepared in a 90 : 10 v/v $H_2O : D_2O$ solution so that the amide NH protons could be observed with solvent suppression by direct presaturation. Correlations from all amide NH protons are shown and the direct NH–αH correlations (as would be observed in COSY) are labeled according to the parent residue. All other correlations result from the extended transfer into the side-chain protons and assist with the identification of the corresponding amino acids. As an example, correlations extending to four vicinal transfer steps may be observed for leucine (L) residues associating NH and δMe resonances. TOCSY has enjoyed very widespread application to assignments of this type since its introduction to high resolution NMR analysis.

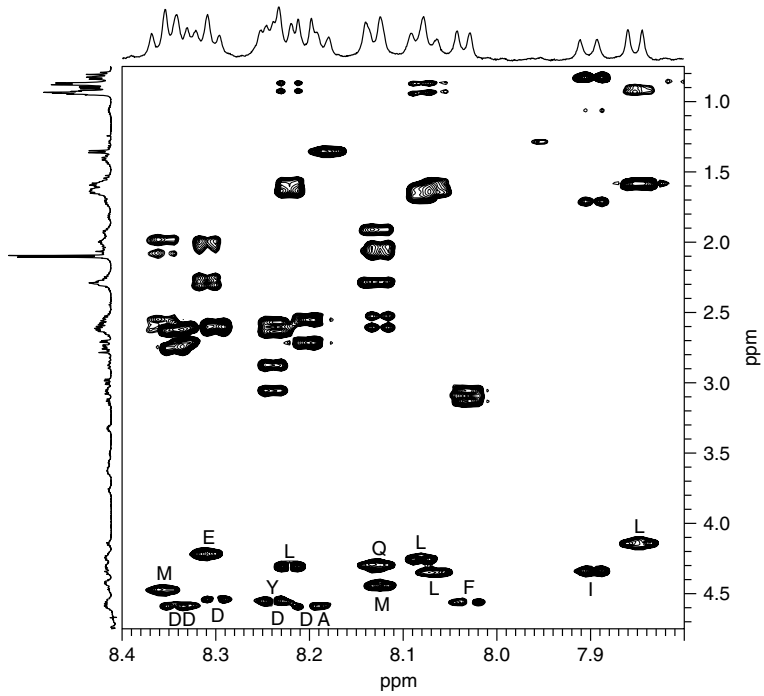

Figure 16.12. A region of the 500-MHz 2D TOCSY ($\tau_m = 80$ ms) of the 19 amino-acid peptide (biotin)-DLDLEMLAPYIPMDDDFQL in 90 : 10 H_2O : D_2O showing extended NH correlations. The vicinal NH–αH correlations are labeled according to the parent amino-acid residue.

The 1D variant of TOCSY now also finds increasing use in the analysis and structure elucidation of smaller organic molecules where specific information may be required. 1D TOCSY allows this to be extracted in a time-efficient manner and with high spectral resolution. The 1D TOCSY data shown in Figure 16.13 illustrate this approach for the analysis of the diterpene structure **2** in which sections of its spectrum are effectively isolated within each trace, allowing these to be correlated with the structure. Furthermore, it becomes possible to reveal multiplet structures that may be partially overlapped or even completely hidden in the conventional 1D proton spectrum so that their structure becomes amenable to detailed analysis. This is most apparent for the *e* and ε proton resonances shown in Figure 16.13, which are coincident in spectrum (a) yet become fully exposed in the TOCSY edited traces (b) and (c). The use of the zero-quantum suppression described in 16.3.4 proves to be especially valuable when undistorted multiplet structures are desired.

A further application of the 1D experiment is in the isolation of the proton (sub)spectrum belonging to a single component contained in a complex mixture,[21] thus providing a form of "purification by NMR". This can be desirable when chromatographic purification of the mixture is undesirable or otherwise impractical. The application requires that a suitable target resonance for the compound of interest can be identified and that an appropriate spin coupling network exists to be exploited within the compound. This concept is illustrated by the identification of the enzymatically produced compound **3** in a crude biosynthetic incubation mix (Figure 16.14). The use of a long 150 ms DIPSI-2 isotropic mixing period provides the complete spectrum of the product from the initially targeted single resonance, devoid of the complicating peaks arising from the incubation starting materials, cofactors, solution buffers, and so on. The very dilute solutions often provided by enzymatic incubations may prevent the acquisition of the full 2D TOCSY experiment, as seen in this example, whereas the 1D

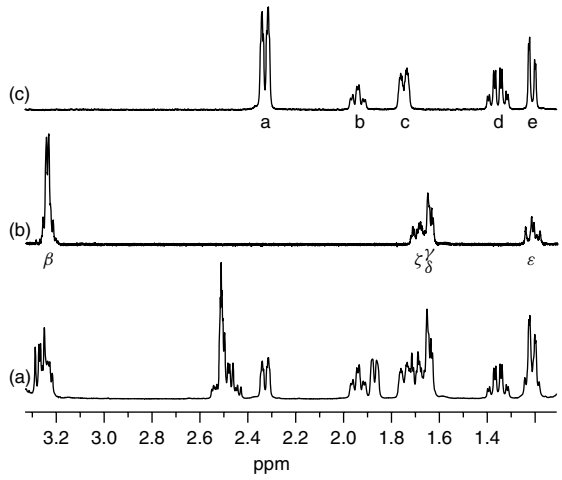

Figure 16.13. The 500 MHz 1D selective TOCSY (τ_m = 80 ms) traces of the diterpene 2 in d_6-DMSO recorded with the sequence shown in Figure 16.7 incorporating the zero-quantum suppression scheme described in 16.3.4.2 and parameters as for Figure 16.10. The reference 500-MHz ^{1}H spectrum is shown in (a) with target resonances for selective excitation of OHα for (b) (at 5.1 ppm; not shown) and Ha for (c).

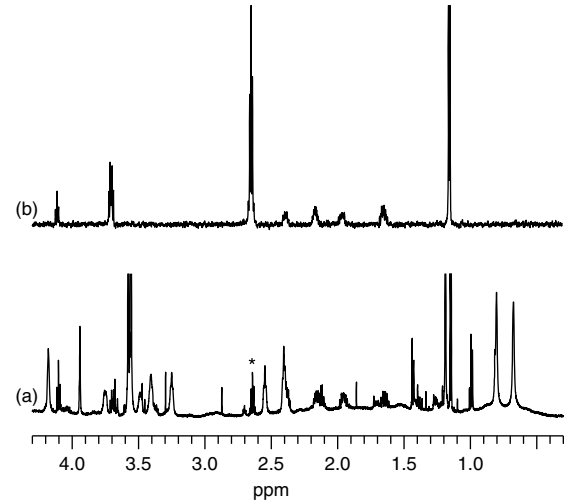

Figure 16.14. The use of 500 MHz 1D selective TOCSY (τ_m = 150 ms) to extract the complete spectrum of 3 in a crude biosynthetic incubation mixture. (a) Incubation mix showing selected target resonance (asterisk) and (b) the isolated resonances of 3 revealed in 1D TOCSY.

variant may provide adequate signal-to-noise ratio in a reasonable time.

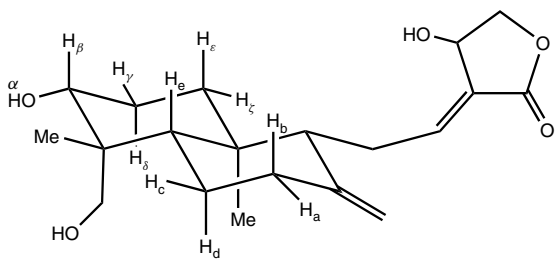

2

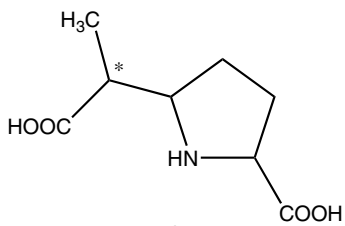

3

In conclusion, we note that the TOCSY mixing element may also be used as an extension to other 2D experiments to enhance their information content. In this way, the correlation information associated with the parent experiment may be further transferred through TOCSY mixing to other protons in the system. Thus, for example, the addition of a mixing period to a proton–carbon HSQC to form the HSQC-TOCSY experiment transfers the initial ^{1}H–^{13}C correlation peak to neighboring protons, thus spreading this information along the proton dimension at each carbon chemical shift.[22] This provides, in effect, ^{13}C-separated total correlation data, which can prove useful for the analysis of extensively crowded spectra. Alternatively, the 1D TOCSY may be used to reveal hidden multiplets (as described above), which may then become suitable targets for a second selective experiment stage, leading to concatenated sequences such as 1D-TOCSY-NOESY.[23,24] Other combinations may also be conceived, but a fuller discussion of these and other hyphenated possibilities is beyond the scope of this article. These will tend to find use in the solution of specific and more unusual problems, whereas the pure TOCSY experiment enjoys very widespread use and serves as a primary technique in structure elucidation.

RELATED ARTICLES IN THE ENCYCLOPEDIA OF MAGNETIC RESONANCE

Carbohydrates and Glycoconjugates

Composite Pulses

Cross Polarization in Solids

Field Gradients and Their Application

Nuclear Overhauser Effect

Peptides and Polypeptides

Phase Cycling

Polarization Transfer Experiments via Scalar Coupling in Liquids

Radiofrequency Pulses: Response of Nuclear Spins

Selective Hartmann–Hahn Transfer in Liquids

Selective Pulses

REFERENCES

1. L. Braunschweiler and R. R. Ernst, *J. Magn. Reson.*, 1983, **53**, 521–528.
2. D. G. Davis and A. Bax, *J. Am. Chem. Soc.*, 1985, **107**, 2820–2821.
3. A. Bax and D. G. Davis, *J. Magn. Reson.*, 1985, **65**, 355–360.
4. M. H. Levitt, R. Freeman, and T. Frenkiel, *J. Magn. Reson.*, 1982, **47**, 328–330.
5. A. J. Shaka, J. Keeler, and R. Freeman, *J. Magn. Reson.*, 1983, **53**, 313–340.
6. A. J. Shaka, J. Keeler, T. Frenkiel, and R. Freeman, *J. Magn. Reson.*, 1983, **52**, 335–338.
7. S. P. Rucker and A. J. Shaka, *Mol. Phys.*, 1989, **68**, 509–517.
8. A. J. Shaka, C. J. Lee, and A. Pines, *J. Magn. Reson.*, 1988, **77**, 274–293.
9. M. Rance, *J. Magn. Reson.*, 1987, **74**, 557–564.
10. R. Bazzo and I. D. Campbell, *J. Magn. Reson.*, 1988, **76**, 358–361.
11. C. Griesinger and R. R. Ernst, *Chem. Phys. Lett.*, 1988, **152**, 239–247.
12. G. Bodenhausen, R. Freeman, and D. L. Turner, *J. Magn. Reson.*, 1977, **27**, 511–514.
13. J. Cavanagh, W. J. Chazin, and M. Rance, *J. Magn. Reson.*, 1990, **87**, 110–131.
14. O. W. Sørensen, M. Rance, and R. R. Ernst, *J. Magn. Reson.*, 1984, **56**, 527–534.
15. M. J. Thrippleton and J. Keeler, *Angew. Chem. Int. Ed.*, 2003, **42**, 3938–3941.
16. C. Griesinger, G. Otting, K. Wüthrich, and R. R. Ernst, *J. Am. Chem. Soc.*, 1988, **110**, 7870–7872.
17. J. Cavanagh and M. Rance, *J. Magn. Reson.*, 1992, **96**, 670–678.
18. U. Kerssebaum, R. Markert, J. Quant, W. Bermel, S. J. Glaser, and C. Griesinger, *J. Magn. Reson.*, 1992, **99**, 184–191.
19. J. Briand and R. R. Ernst, *Chem. Phys. Lett.*, 1991, **185**, 276–285.
20. M. Kadkhodaie, T. L. Hwang, J. Tang, and A. J. Shaka, *J. Magn. Reson. (A)*, 1993, **105**, 104–107.
21. G. J. Sharman, *Chem. Commun.*, 1999, 1319–1320.
22. D. G. Davis, *J. Magn. Reson.*, 1989, **84**, 417–424.
23. M. J. Gradwell, H. Kogelberg, and T. A. Frenkiel, *J. Magn. Reson.*, 1997, **124**, 267–270.
24. H. Hu, S. A. Bradley, and K. Krishnamurthy, *J. Magn. Reson.*, 2004, **171**, 201–206.